Next, we compared the reactivity of 4G8 with commercially available anti-SLA class I Abs 74-11-10, PT85A, H17A, H58A to PB from outbred domestic pigs. As shown in Figure 2, flow-cytometrical analysis demonstrated that the reactivity of 74-11-10 and PT85A to the porcine PB was similar to that of 4G8. Although multiple samples from individual animals were tested, all of these MAbs always revealed a pan leukocyte positive staining pattern. In contrast, H17A did not react with the domestic porcine PB samples (data not shown), indicating that H17A is polymorphic in pigs. H58A, exhibited variable reactivity from one animal to another (data not shown). This data indicates that the reactivity of H17A and H58A is different from that of 4G8.

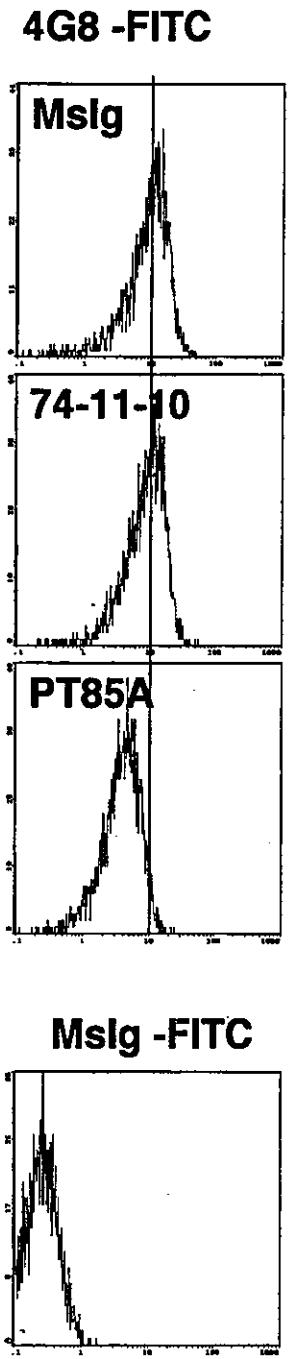

FIG. 3. Competition binding assay using flow cytometry. 4G8 continued to react with porcine PB leukocytes that had been saturated with commercially available MAbs (74-11-10 and PT85A). MsIg-FITC was used as a negative control.

To determine whether the epitope recognized by 4G8 was the same as that of 74-11-10 and PT85A, we examined whether 4G8 could still bind to the cells after the cells had been saturated with 74-11-10 or PT85A. As shown in Figure 3, 4G8 continued to react with PB leukocytes that had been saturated with 74-11-10 or PT85A. These results indicate that 4G8 recognizes a novel epitope distinct from those recognized by 74-11-10, PT85A, H17A and H58A. MHC class I molecules are extremely polymorphic, and polymorphism often occurs in the $\alpha 1$ domain, or the $\alpha 2$ domain, but the $\alpha 3$ domain is nonpolymorphic.[4] 74-11-10 and PT85A have been reported to require the PD1 $\alpha 1/\alpha 2$ domains, but not the $\alpha 3$ domain, to exhibit reactivity.[1] A precise analysis to clarify which domain is recognized by 4G8 is now underway.

Analysis of 4G8 using immunohistochemistry

We examined whether 4G8 could be used to immunostain frozen sections. As shown in Figure 4, 4G8 produced high-quality immunostaining results when used on frozen sections. In thymus tissues, 4G8 produced a dense and diffuse staining pattern in the medullar region and a lighter, scattered staining pattern in the cortex, suggesting that SLA class I molecules are mainly expressed on mature thymocytes in the medulla, but not on immature thymocytes in the cortex. In spleen, lymph node, kidney and liver tissues, 4G8 produced an ubiquitous staining pattern, as shown in Figure 4. These results demonstrate that 4G8 can be effectively used to immunostain frozen sections. Therefore, 4G8 may be a useful reagent for immunopathology studies and improving our general understanding of the porcine immune system.

In conclusion, a novel MAb, 4G8, that recognizes the SLA class I α chain has been identified and used to produce high-quality immunostaining results on tissues sections. 4G8 is expected to become a useful tool for investigating the immune system of domestic pigs.

ACKNOWLEDGMENTS

We thank M. Sone and S. Yamauchi for their excellent secretarial work. This research was supported in part by Health and Labor Sciences Research Grants from the Ministry of Health, Labor and Welfare of Japan and MEXT (KAKENHI 15019129, JSPS. KAKENHI 15390133 and 15590361). Support was also provided by a grant from the Japan Health Sciences Foundation for Research on Health Sciences Focusing on Drug Innovation and a grant from the Sankyo Foundation of Life Science.

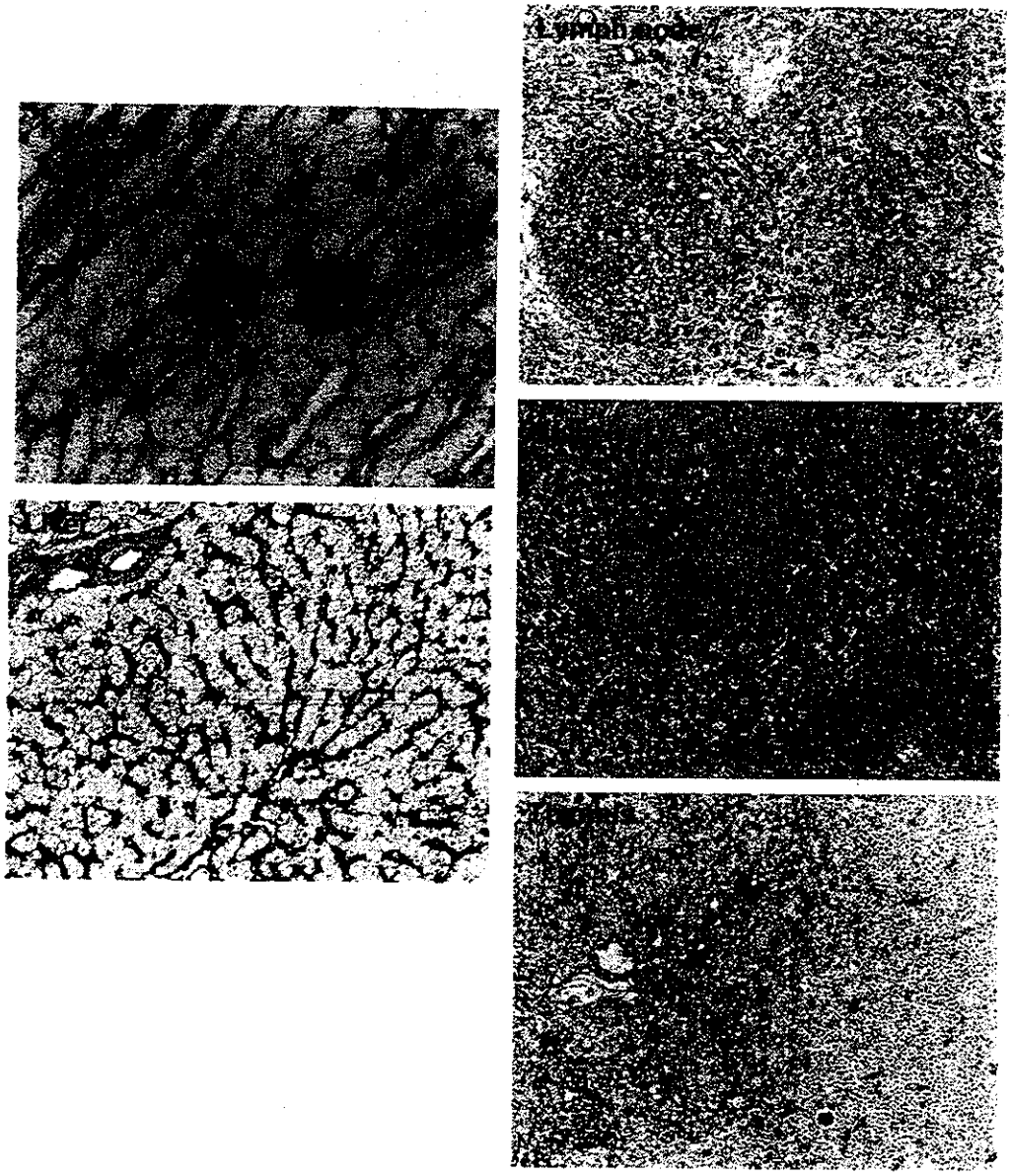

FIG. 4. Reactivity of 4G8 on frozen sections of porcine tissues. Frozen sections of porcine thymus, spleen, lymph node, kidney, and liver tissues were stained with 4G8 using immunohistochemistry.

REFERENCES

1. DerSimonian H, Pan L, Yatko C, Rodrigue-Way A, Johnson E, and Edge AS: Human anti–porcine T cell response: blocking with anti–class I antibody leads to hyporesponsiveness and a switch in cytokine production. J Immunol 1999;162:6993–7001.
2. Fujimoto J, Ishimoto K, Kiyokawa N, Tanaka S, Ishii E, and Hata J: Immunocytological and immunochemical analysis on the common acute lymphoblastic leukemia antigen (CALLA): evidence that CALLA on ALL cells and granulocytes are structurally related. Hybridoma 1988;7:227–236.
3. Maruyama K, and Sugano S: Oligo-capping: a simple method to replace the cap structure of eukaryotic mRNAs with oligoribonucleotides. Gene 1994;138:171–174.
4. Sullivan JA, Oettinger HF, Sachs DH, and Edge AS: Analysis of polymorphism in porcine MHC class I genes: alterations in signals recognized by human cytotoxic lymphocytes. J Immunol 1997;159: 2318–2326.

Address reprint requests to:
Junichiro Fujimoto, Ph.D.
Department of Developmental Biology
National Research Institute for Child Health and Development
3-35-31, Taishido, Setagaya-ku
Tokyo 154-8567, Japan

E-mail: jfujimoto@nch.go.jp

Received for publication February 27, 2004. Accepted for publication March 24, 2004.

Available online at www.sciencedirect.com
SCIENCE DIRECT
Veterinary Immunology and Immunopathology 103 (2005) 113–127
Veterinary immunology and immunopathology
www.elsevier.com/locate/vetimm

Characterization of new monoclonal antibodies against porcine lymphocytes: molecular characterization of clone 7G3, an antibody reactive with the constant region of the T-cell receptor δ-chains

W.-R. Tang[a], N. Shioya[a], T. Eguchi[c], T. Ebata[a], J. Matsui[a], H. Takenouchi[a], D. Honma[c], H. Yasue[c], Y. Takagaki[d], S. Enosawa[b], M. Itagaki[a], T. Taguchi[a], N. Kiyokawa[a], H. Amemiya[b], J. Fujimoto[a,*]

[a]*Department of Developmental Biology, National Research Institute for Child Health and Development, 3-35-31 Taishido, Setagaya-ku, Tokyo 154-8567, Japan*
[b]*Department of Innovative Surgery, National Research Institute for Child Health and Development, 3-35-31 Taishido, Setagaya-ku, Tokyo 154-8567, Japan*
[c]*Genome Research Department, National Institute for Agrobiological Science, 2-1-2 Kannondai, Tsukuba, Ibaraki 305-8602, Japan*
[d]*Department of Molecular Medicine, Kitasato University School of Medicine, 1-15-1 Kitasato, Sagamihara Kanagawa 288-8555, Japan*

Received 14 November 2003; received in revised form 9 July 2004; accepted 26 August 2004

Abstract

A battery of mouse monoclonal antibodies (mAbs) reactive with porcine peripheral blood (PB) leukocytes was generated. Among the mAbs, 6F10 was found to react probably with cluster of differentiation (CD)8 α-chain, while 7G3 and 3E12 were found to recognize γδ T-cells, as revealed by two-color flow cytometric and immunoprecipitation studies. 7G3 was shown to react with the constant (C) region of the T-cell receptor (TCR) δ-chain by the following facts: (1) 7G3 immunoprecipitated full-length TCR δ-chain protein fused with glutathione S-transferase (GST) produced by *Escherichia coli* and (2) 7G3 reacted with TCR δ-chain expressing Cos-7 cells transfected with either full-length or N-terminal deleted mutant cDNA, but did not react with Cos-7 cells transfected with C-terminal deleted mutant TCR δ-chain cDNA. All three mAbs produced high-quality immunostaining results on frozen sections, revealing a distinct distribution of γδ T-cells and $CD8^+$ cells. This report precisely

Abbreviations: CD, cluster of differentiation; PB, peripheral blood; C region, constant region; PE, phycoerythrin; GST, glutathione S-transferase; HRP, horseradish peroxidase

* Corresponding author. Tel.: +81 3 3487 9669; fax: +81 3 3487 9669.
E-mail address: jfujimoto@nch.go.jp (J. Fujimoto).

0165-2427/$ – see front matter
doi:10.1016/j.vetimm.2004.08.018

characterizes mAbs against porcine TCR for the first time, facilitating molecular biological investigations of the porcine immune system.

Keywords: Pig; T lymphocytes; Antibodies; T-cell receptors

1. Introduction

Considerable interest has been focused on the immunobiology of the pig, since this animal is regarded as a candidate for organ supply in transplantation medicine. From an animal husbandry point of view, understanding the immune systems of livestock animals enables the food supply to be improved through the manipulation of immunity-related genes. In this regard, workshops on porcine cluster of differentiation (CD) have been conducted and reports are published periodically. Several mAbs have been established, but the number of mAbs for porcine leukocyte Ags remains small compared with those for murine and human systems; furthermore, most of the mAbs that have been established for porcine systems require a more detailed characterization (Haverson et al., 2001a,b).

We thus attempted to develop new mAbs that could be used to analyze the porcine immune system. This manuscript describes the development of various mAbs that are reactive with porcine leukocytes. In particular, one mAb designated as 7G3 was confirmed to react with the constant (C) region of the recombinant TCR δ-chain. This report is the first description of a mAb against porcine TCR δ-chain, whose characterization was confirmed using molecular biology techniques. The utilization of the newly developed mAbs in the immunostaining of tissue sections was also demonstrated.

2. Materials and methods

2.1. Animals and tissues

Landrace or (Landrace × Large White) F1 pigs were used in the study. Peripheral blood (PB) and tissues were obtained from anesthetized animals and processed using conventional techniques, PB was collected in tubes containing acid citric buffer to avoid coagulation. Tissues were immediately snap frozen and kept in a deep freezer until use. In some experiments, thymus tissue was minced with scissors to generate a cell suspension. A viable thymocyte suspension was then prepared using Ficoll–Paque (Immuno-Biological Laboratories Co. Ltd., Takasaki-shi, Gunma-ken, Japan) gradient centrifugation.

2.2. Monoclonal antibodies

PB leukocytes were isolated from PB by RBC lysis with an NH_4Cl lysis buffer followed by centrifugation at 1500 rpm for 10 min. After washing twice in PBS, approximately 1×10^8 cells were injected into the abdominal cavity of an 8-week-old female Balb/c mouse. Two boost injections were performed at 2-week intervals. Four days after the last boost injection, splenocytes were fused with P3U1 mouse myeloma cells and incubated in hypoxanthine and thymidine (HAT) medium. Supernatants of growing hybridomas were screened on porcine PB leukocytes using flow cytometry, and clones that secreted Abs which were reactive with porcine PB leukocytes were subcloned twice using limited dilutions. The clones were grown in the abdominal cavity of Pristane-treated Balb/c mice and ascites samples were subsequently obtained. Purification of the mAbs was performed using a Protein-G column (Bio-Rad Laboratories, Hercules, CA). After purification, the mAbs were either biotinylated or conjugated with FITC, as previously described (Fujimoto et al., 1988). Commercially available mAbs against porcine CD2 (clone MSA4), CD3 (8E6), CD4 (74-12-4, also known as PT4), CD5 (PG114A), CD8 α-chain (76-2-11, also known as PT8), CD8 β-chain (PG164A), γδ T-cells (PT79A, PG92A, PG94A, PGBL22A and 86D) and CD21 (BB6-11C9) were obtained from Veterinary Medical Research and Development Inc. (Pullman, WA).

2.3. Flow cytometry and immunohistochemistry

The flow cytometry analyses of the mAbs were performed as follows. Briefly, an aliquot of porcine PB

leukocytes or thymocytes was incubated with an appropriate amount of mAb for 30 min at 4 °C. After washing with PBS, the cells were incubated with either FITC-conjugated or phycoerythrin (PE)-conjugated goat anti-mouse Abs (Jackson Laboratory Inc., West Grove, PA) for 30 min at 4 °C. The cells were then washed with PBS and analyzed using an EPICS XL analyzer (Beckman/Coulter Inc., Westbrook, MA). In some experiments, two-color flow cytometry was performed to distinguish between the newly established mAbs and commercially available mAbs. Briefly, porcine PB leukocytes were incubated first with unconjugated mAbs and then with PE-labeled secondary Abs, as described above. The free-binding sites of the second Abs were blocked with an excess amount of unrelated mouse Ab, and the cells were treated with FITC-conjugated mAbs.

The reactivity of the mAbs in tissues was analyzed using frozen sections and immunohistochemistry. Briefly, porcine tissues were snap-frozen in optimal cutting temperature (OCT) compounds, and frozen sections were made using a cryostat apparatus. The sections were fixed in acetone for 15 min at 4 °C. After washing in PBS and blocking with normal rabbit serum, the sections were incubated with mAbs at appropriate dilutions for 30 min at room temperature. The sections were then washed with PBS and incubated with horseradish peroxidase (HRP)-conjugated rabbit anti-mouse Abs (Jackson) for 30 min at room temperature. After washing with PBS, color development was performed in a diaminobenzidine solution (10 mM in 0.05 M Tris–HCl, pH 7.5) with 0.003% H_2O_2.

2.4. Immunoprecipitation

Porcine PB leukocytes were biotinylated and lysed in a lysis buffer, as previously described (Takada et al., 1995). After centrifugation for 30 min at 15,000 rpm and 4 °C, the supernatant was removed and used for the immunoprecipitation. Cell lysates were first incubated with Protein-G agarose beads (Boehringer Mannheim Biochemica, Mannheim, Germany) to remove non-specific binding proteins, and aliquots were incubated with the mAbs followed by Protein-G beads. After washing, the immunoprecipitates were loaded onto SDS-PAGE and transferred to a nitrocellulose membrane. The immunoprecipitates were then reacted with HRP-conjugated avidin and washed. Finally, HRP activity was visualized using chemiluminescence (ECL, Amersham Life Science, Buckinghamshire, UK), as described elsewhere.

2.5. Cloning and expression of porcine TCR cDNA

cDNA libraries of $7G3^+$ PB leukocytes and $6F10^+$ PB leukocytes were constructed. Porcine PB lymphocytes labeled with FITC-7G3 Ab were incubated with magnetic-activated cell sorting (MACS) beads conjugated with anti-FITC Ab (Miltenyi Biotec GmbH, Bergisch Gladbach, Germany) and loaded onto an AutoMACS cell separator (Miltenyi Biotec). $7G3^+$ cells were positively selected, and a cDNA library was constructed using the oligo-capping method (Maruyama and Sugano, 1994) and plasmid vector pME18S-FL3, which contains the SR-α promoter for expression in mammalian cells, FITC-6F10 was added to the $7G3^-$ pass-through fractions and labeled. These cells were also positively selected by AutoMACS and used for the cDNA library construction. Out of several thousand clones sequenced from both cDNA libraries, eight clones (four TCR δ-chain clones [D1 through D4], two TCR α-chain clones [A1 and A2], one TCR γ-chain clone [G], and one TCR β-chain clone [B]) that exhibited homologies to known TCR sequences and contained full-length open reading frames were selected. It was confirmed that all of the cDNAs were full length and error-free in comparison with previously published nucleotide sequence of porcine TCRs (Thome et al., 1993). To generate a mammalian cell expression vector for V region of the TCR δ-chain, a termination codon was introduced at nucleotides 343–345 of the TCR δ-chain coding sequence in pME18S-FL3 TCR D4 by site-directed mutagenesis (Quick Change Mutagenesis Kit, Stratagene) (see Fig. 5). To generate a mammalian cell expression vector for the C region of the TCR δ-chain, an additional *Bam*HI site was introduced at nucleotides 436–441 of the TCR δ-chain coding sequence in pME18S-FL3 TCR D4, and the nucleotide fragment 50–436 of the TCR δ-chain coding sequence was deleted by *Bam*HI digestion followed by self ligation (see Fig. 5). For the bacterial expression of the glutathione S-transferase (GST)-fusion recombinant

TCR δ-chain protein, *Bam*HI and the blunt-ended *Sac*I fragment of the TCR δ (D4) cDNA were introduced to the pGEX-6P-1 (Pharmacia Biotech, Uppsala, Sweden) vector at the *Bam*HI and *Sma*I sites.

cDNA coding for the TCRs under the SRα promoter was introduced into Cos-7 cells by lipofection (LIPOFECTAMIN, Invitrogen, Groningen, The Netherlands); after 3 days, the cells were stained with 7G3 mAb. Recombinant TCR proteins with a GST-fusion form were immunoprecipitated with 7G3 mAb and analyzed by SDS-PAGE.

3. Results and discussion

3.1. Development of mAbs reactive with porcine PB leukocytes

From one hybridization experiment, 45 hybridoma clones were established. The mAbs produced by these clones reacted differently to the porcine PB leukocytes, as revealed by flow cytometry, and were classified into several groups according to their pattern of reactivity (Table 1). Among them, mAbs 6F10, 7G3 and 3E12, which reacted with lymphocyte subpopulations were extensively analyzed.

mAb 6F10 reacted with 49.0% (range 40.3–60.5%; $n = 5$) of the PB lymphocytes (Table 2). The histogram profiles always displayed bright and dull peaks (Fig. 1). Since this pattern is typical of CD8, a two-color analysis was performed using previously established CD3 and CD8 mAbs. As shown in Fig. 1A, most of the cells stained positive for both 6F10 and CD3, but a small population of $CD3^-$ $6F10^+$ cells were also identified. A two-color analysis using the CD8 α-chain mAb showed that 6F10 and CD8 α-chain reacted in identical cell populations, since the histograms could be aligned in a diagonal fashion. On the other hand, a two-color analysis with CD8 β-chain indicated that the mAb against CD8 β-chain reacted only with a bright population of $6F10^+$ cells. In thymocytes, a similar 6F10 staining pattern was obtained (Fig. 1B). Thus, $6F10^+$ cells were mostly found in $CD3^+$ cells, and the two-color histograms for 6F10 and CD8 α-chain were aligned in a diagonal fashion. From these results, we concluded that 6F10 probably recognizes the porcine CD8 α-chain.

mAb 7G3 reacted with 24.7% (range 14.2–32.7%; $n = 5$) of the PB lymphocytes (Table 2). As shown in Fig. 2, a two-color analysis demonstrated that nearly all the $7G3^+$ cells were found in $CD2^+$ and $CD3^+$ cells. On the other hand, the $7G3^+$ cells were always $CD4^-$. The relationship between 7G3-positivity with CD8 α-chain-positivity varied depending on the nature of the sample that was being examined. $7G3^+$CD8 α-$chain^+$ and $7G3^+$CD8 α-$chain^-$ cells were always present, but their proportions differed significantly from sample to sample (see samples #1 and #2 in Fig. 2). Since the $7G3^+$ cells were identified as $CD3^+$ T-cells, we next examined whether $7G3^+$ cells were related to γδ T-cells using previously established mAbs against porcine TCR δ-chain (Fig. 2, right panel). Using five

Table 1
Classification of new monoclonal antibodies defined by their specificities to peripheral blood leukocytes using flow cytometry

Specificity	Clones
Pan-leukocyte	1B4, 1B8, 4G8, 5B6, 5B11, 6F1, 6F2, 7D8, 7G12
Granulocyte	1H2, 3C5, 3F5, 3F11, 5A10, 5E6, 5H7, 6B4, 6B8, 6E10, 6G1, 7H12, 8F2
Lymphocyte subset	2E2, 2H3, 3E12, 5D8, 5G8, 6E12, 6F10, 7G3
Granulocyte and lymphocyte subset	1F4, 2F12, 3D10, 4H9, 5E11, 6A8, 6D10, 6F11, 7C7, 7G1, 7G11, 8A5, 8C1, 8C3, 8H7

Table 2
Reactivities of monoclonal antibodies against porcine peripheral blood lymphocytes

	Pig 1	Pig 2	Pig 3	Pig 4	Pig 5	Mean (%)	S.D.
T-cell							
CD3	73.0	63.9	55.9	52.5	71.4	63.3	9.1
CD4	24.8	24.8	18.0	19.1	25.7	22.5	3.6
CD8α	46.4	54.3	39.1	44.3	42.6	45.3	5.7
CD8β	15.4	23.3	12.7	11.9	17.1	16.1	4.5
6F10	47.5	60.5	40.3	45.3	51.5	49.0	7.6
γδ TCR							
PT79A	15.3	16.5	18.8	12.1	23.5	17.2	4.3
PG92A	10.7	16.5	9.1	4.9	17.1	11.7	5.2
PG49A	13.0	5.2	12.6	12.7	13.4	11.4	3.5
PGBL22A	29.7	16.1	27.0	19.3	32.1	24.8	6.9
86D	4.7	6.2	6.7	8.8	12.9	7.9	3.2
7G3	30.5	14.2	27.2	19.0	32.7	24.7	7.9
3E12	16.2	9.3	16.1	11.6	20.4	14.7	4.3
B cell							
CD21	6.0	10.5	8.1	8.9	5.4	7.8	2.1

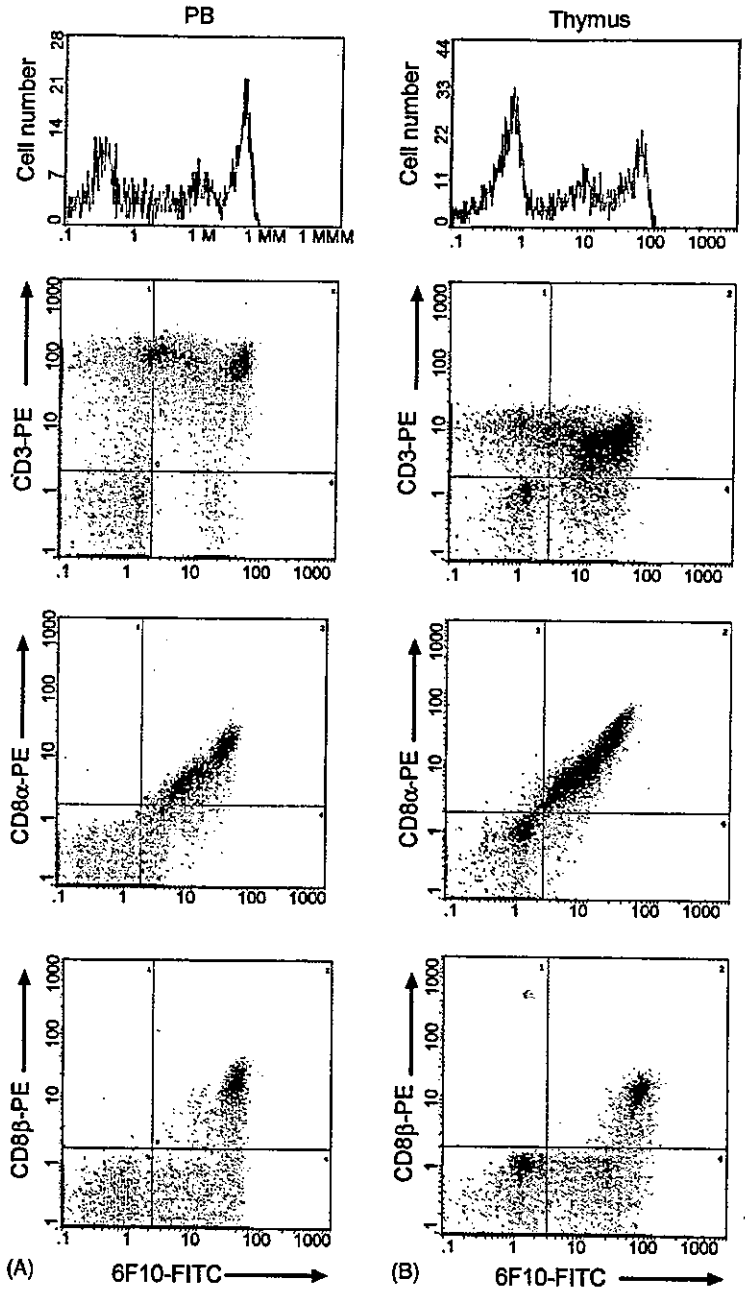

Fig. 1. Two-color staining of porcine peripheral blood lymphocytes and thymocytes using the 6F10 monoclonal antibody and other T-cell markers. Peripheral blood lymphocytes (A) and thymocytes (B) were stained with combinations of FITC-conjugated 6F10 (*X*-axis) and other PE-labeled antibodies (*Y*-axis).

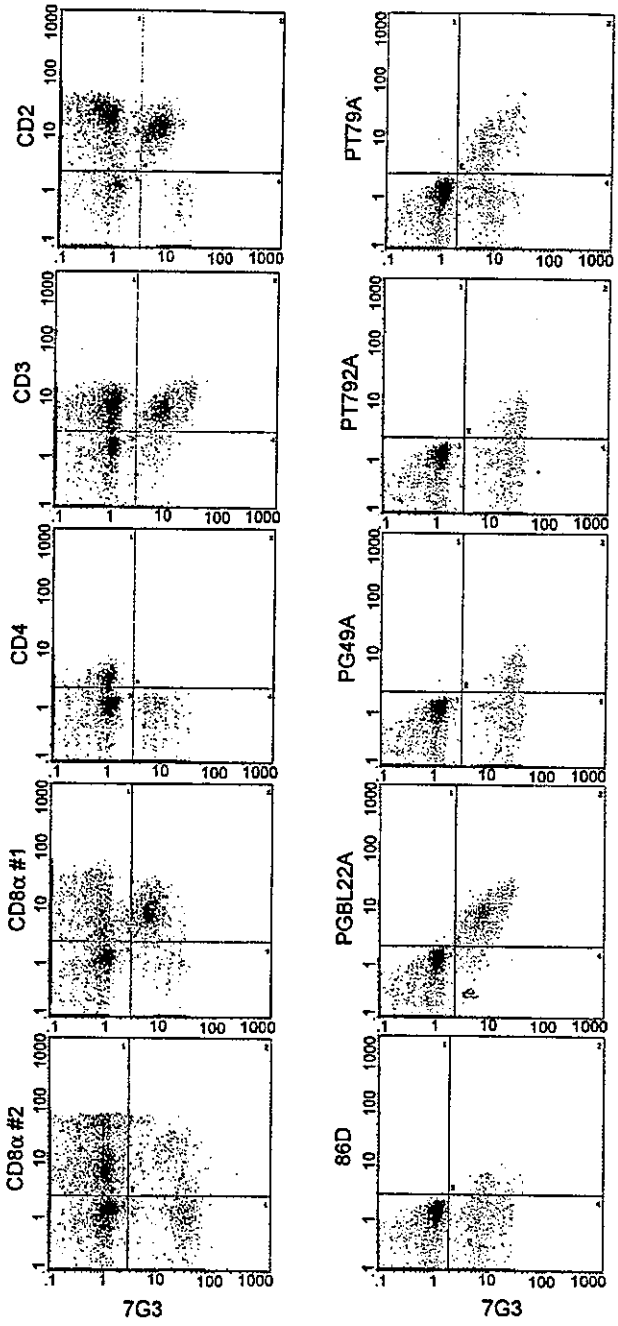

Fig. 2. Two-color staining of porcine peripheral blood lymphocytes using 7G3 and other T-cell markers. Peripheral blood lymphocytes were stained with combinations of FITC-conjugated 7G3 (*X*-axis) and other PE-labeled antibodies (*Y*-axis).

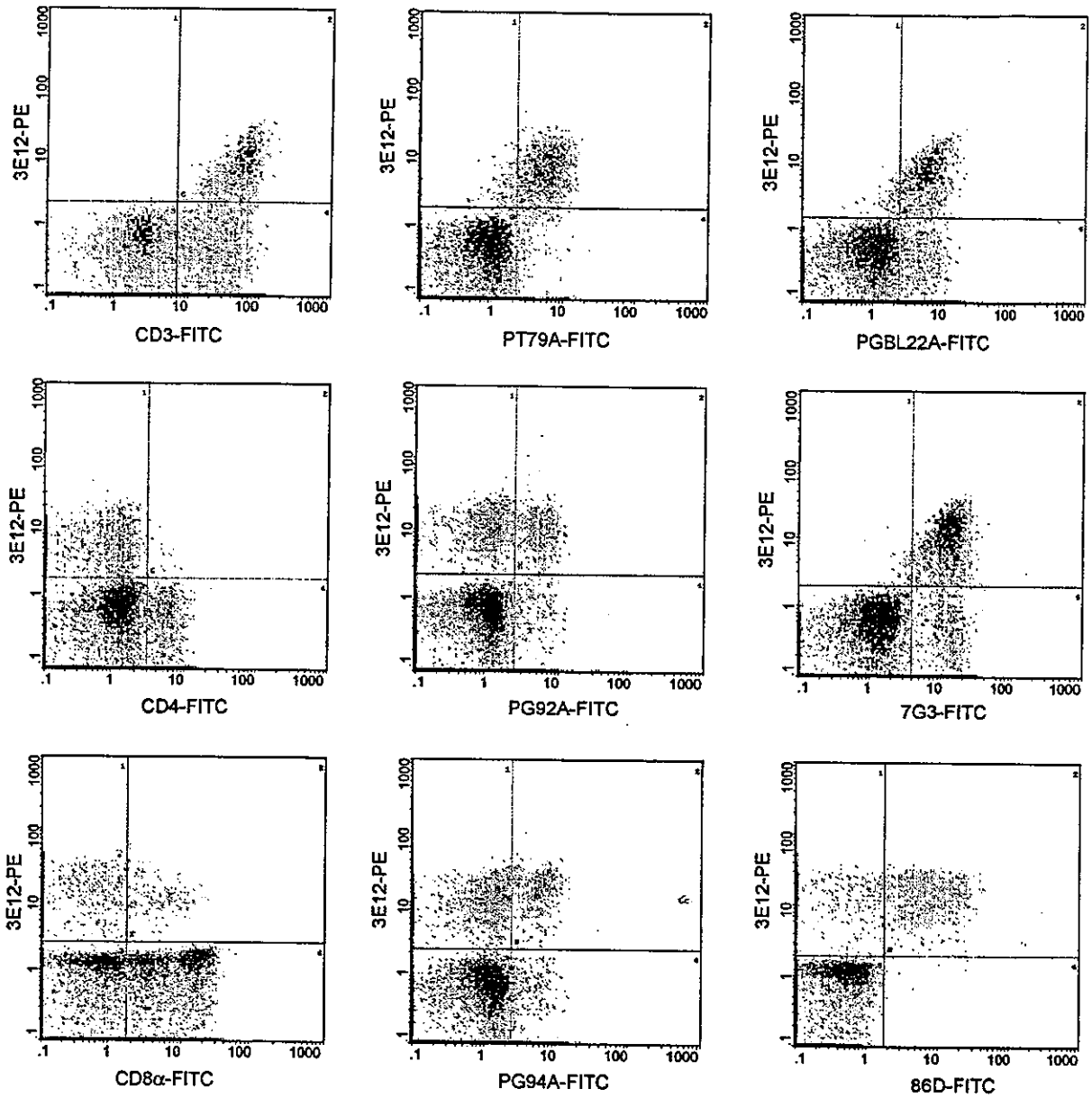

Fig. 3. Two-color staining of porcine peripheral blood lymphocytes using 3E12 and other T-cell markers. Peripheral blood lymphocytes were stained with combinations of PE-conjugated 3E12 (*Y*-axis) and other FITC-labeled antibodies (*X*-axis).

mAbs against γδ T-cells (PT79A, PG92A, PG94A, PGBL22A and 86D), we found that 7G3 always labeled a population of cells that overlapped the population stained by these mAbs against porcine γδ T-cells. Among them, the $7G3^+$ cells were almost identical to those detected by PGBL22A. The reactivity of 7G3 was also examined in porcine thymocytes. Consistent with the results obtained for PB lymphocytes, the staining pattern for 7G3 was almost identical to that for PGBL22A (data not shown).

mAb 3E12 reacted with 14.7% (range 9.3–20.4%; $n = 5$) of the PB lymphocytes (Table 2). As shown in

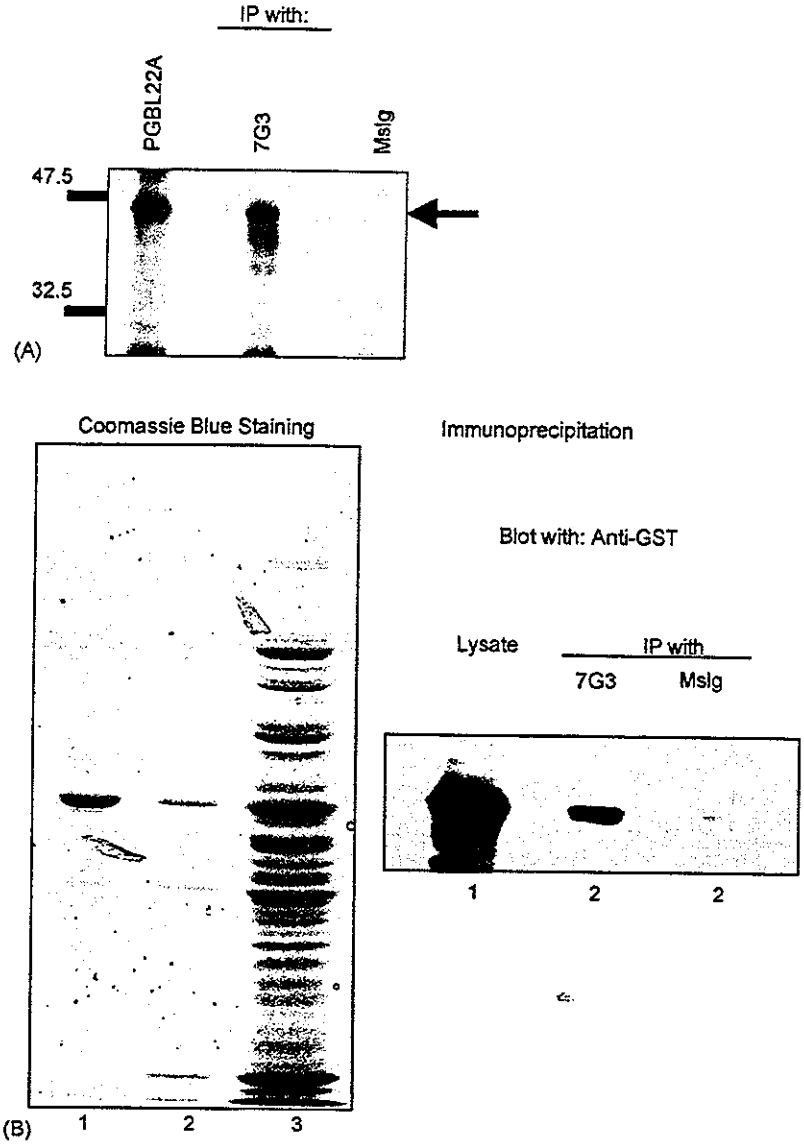

Fig. 4. Immunoprecipitation study using 7G3. (A) Immunoprecipitation was performed using 7G3 or PGBL22A in cell lysates extracted from biotinylated porcine peripheral blood leukocytes. After separation on an SDS-PAGE gel, the proteins were transferred onto a nitrocellulose membrane and probed with peroxidase-conjugated avidin. An unrelated mouse monoclonal antibody (MsIg) was used as a control. (B) GST fusion proteins of the full-length porcine TCR δ-chain were produced in *Eschericha coli* (lane 3). After purification with glutathione sepharose (lane 1), the proteins were eluted with reduced glutathione (lane 2). Each protein was separated by SDS-PAGE in a 10% acrylamide gel and visualized using Coomasie blue-staining. (C) Immunoprecipitation was performed on eluted purified GST fusion TCR δ-chain proteins as described in A followed by immunoblotting with an anti-GST antibody. Lysates of full-length porcine TCR δ-chain were produced in *E. coli* and used as a positive control for the anti-GST antibody. As a negative control, an unrelated mouse monoclonal antibody (MsIg) was used.

Fig. 3, a two-color analysis demonstrated that the staining pattern of 3E12 was similar to that of 7G3. All $3E12^+$ cells were included in the $CD3^+$ cells, but not in the $CD4^+$ cells, and a portion of the $3E12^+$ cells overlapped with the CD8 α-chain$^+$ cells. Further analysis revealed that the $3E12^+$ cells were always included in both $7G3^+$ and $PGBL22A^+$ cells, with approximately two-thirds of the $7G3^+$ cells being

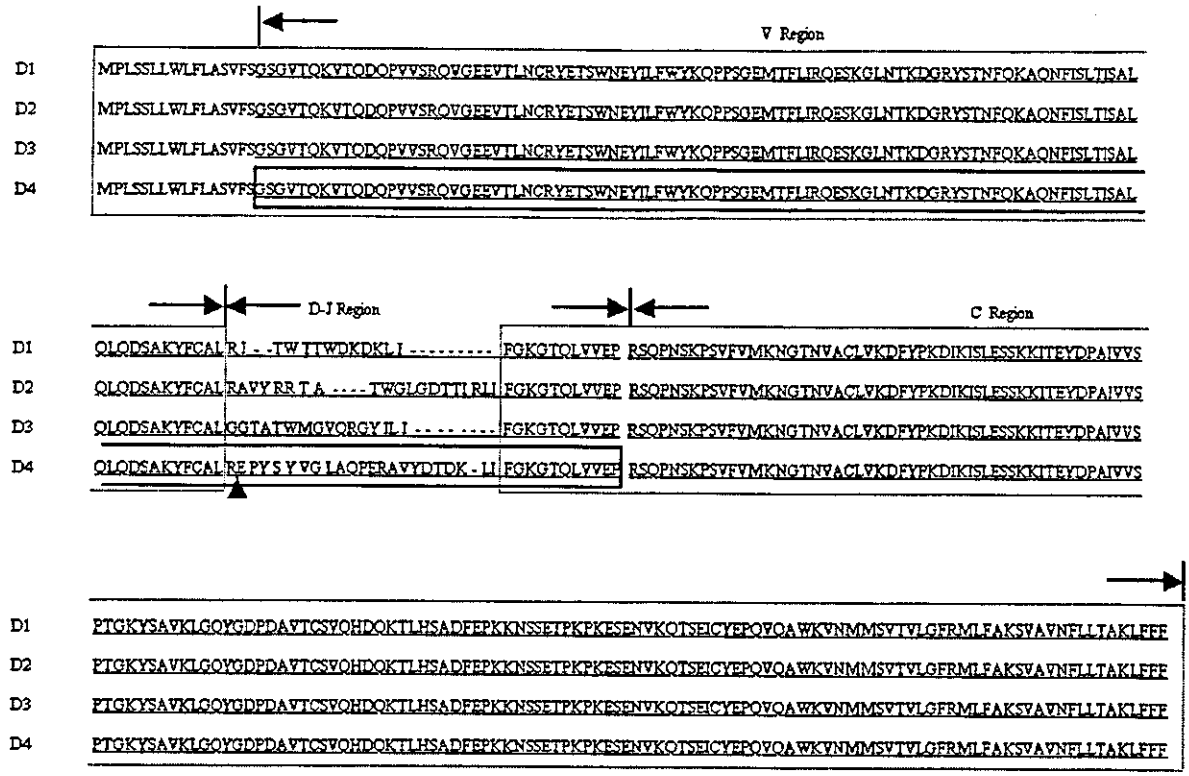

Fig. 5. Schematic presentation of TCR δ-chain cDNA. The nucleotide sequences of the TCR δ-chain cDNAs that were cloned from the 7G3$^+$ cell cDNA library are shown. The arrow-head indicates a termination codon introduced in TCR D4 to generate the TCR D4 V region construct. The solid box indicates the deleted site in the TCR D4 C region construct.

positive for 3E12. The 3E12$^+$ cells were almost identical to those detected by PT79A, and only partially overlapped with either PG92A$^+$ or PG94A$^+$ cells. The above data indicates that 3E12 recognizes a subpopulation of γδ T-cells.

3.2. Reactivity of 7G3 with TCR δ-chain protein

From the biotinylated cell lysates of PB lymphocytes, 7G3 immunoprecipitated a protein with a molecular weight of approximately 40 kDa under reducing conditions (Fig. 4A). A side-by-side comparison revealed that mAb PGBL22A, which has been reported to detect the TCR δ-chain, produced a band with an identical molecular weight.

To confirm that 7G3 reacted with TCR δ-chain, 7G3 was challenged to react with recombinant forms of the TCR δ-chain protein. In our cDNA libraries prepared from 7G3$^+$ cells and 6F10$^+$ cells, one TCR β-chain clone (TCR B), one TCR γ-chain clone (TCR G), two TCR α-chain clones (TCR A1 and A2) and four TCR δ-chain clones (TCR D1 through D4) (Fig. 5) full-length cDNAs were identified. These cDNAs were inserted into mammalian expression vector pME18S-FL3 and transfected into Cos-7 cells. After culturing for three days, the cells were stained with 7G3 using an immunohistochemical method. No staining was observed when the TCR β-chain (Fig. 6A), TCR α-chain or TCR γ-chain cDNAs were transfected (data not shown), but the Cos-7 cells that were transfected with one of the four different TCR δ-chain cDNAs stained positive for 7G3 (Fig. 6A, Table 3). An identical staining pattern to that of 7G3 was obtained when mAb PGBL22A was used (Table 3).

The above results prompted us to examine the reactivity of 7G3 with TCR δ-chain recombinant protein. For this purpose, we first produced a full-

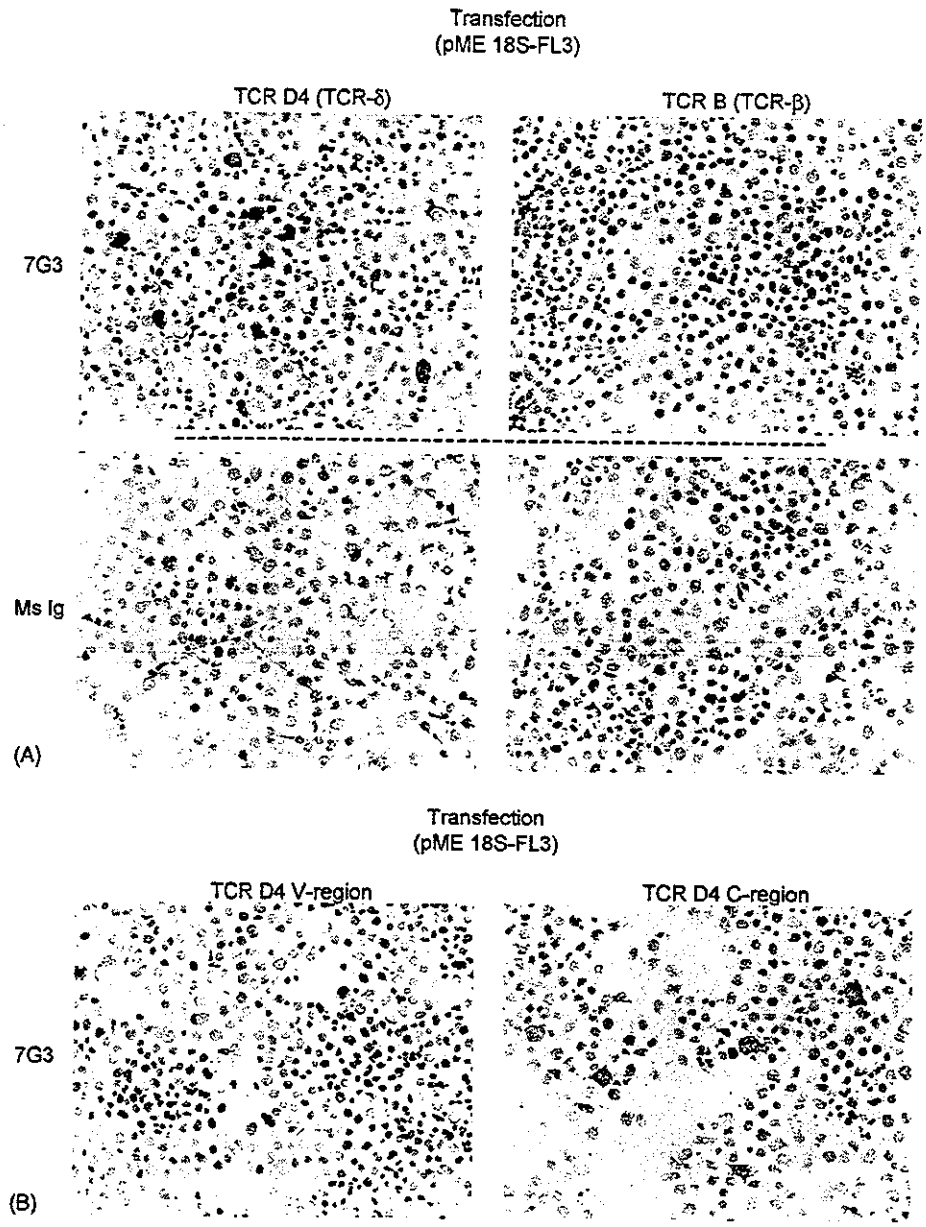

Fig. 6. Reactivity of 7G3 on Cos-7 cells transfected with TCR δ-chain cDNA. (A) Mammalian expression vectors containing either TCR δ-chain (TCR D4) or TCR β-chain (TCR B) were introduced into Cos-7 cells, and the cells were stained with 7G3 or a control antibody. (B) Expression vectors for the TCR δ-chain mutant that completely lack either the C region (TCR D4 V region) or the V region (TCR D4 C region) were introduced into Cos-7 cells, and the cells were stained with 7G3 or a control antibody.

length TCR δ-chain recombinant protein fused with GST in bacteria. As shown in Fig. 4B, a full-length TCR δ-chain-GST fusion protein with a molecular weight of 60 kDa was effectively produced (lane 3) and purified using glutathione beads (lanes 1 and 2). An immunoprecipitation experiment using 7G3 and the recombinant full-length TCR δ-chain-GST fusion protein, followed by immunoblotting with anti-GST

Table 3
Reactivities of monoclonal antibodies against Cos-7 cells transfected with various types of porcine TCR cDNA

	TCR D1	TCR D2	TCR D3	TCR D4	TCR A1	TCR A2	TCR G	TCR B
7G3	+	+	+	+	–	–	–	–
PGBL22A	+	+	+	+	–	–	–	–
PT79A	–	–	–	–	–	–	–	–
PG92A	–	–	–	–	–	–	–	–
PG94A	–	–	–	–	–	–	–	–
86D	–	–	–	–	–	–	–	–
3E12	–	–	–	–	–	–	–	–

Ab, clearly indicated that 7G3 reacted with the full-length TCR δ-chain protein (Fig. 4C).

Next, we determined whether 7G3 reacts with the C region or the V region of the TCR δ-chain. GST protein fused with the V region of the TCR δ-chain was successfully produced in bacteria, but was not reactive with 7G3 (data not shown). Since we failed to produce the C region of the TCR δ-chain protein in bacteria, we attempted to use a mammalian expression system and a deletion mutant of the TCR D4 clone. As shown in Fig. 6B, 7G3 reacted with the Cos-7 cells in which the N-terminal deletion mutant of the TCR D4 clone, containing the C region of the TCR δ-chain, was expressed. On the other hand, 7G3 did not react with Cos-7 cells in which the C-terminal deletion mutant of the TCR D4 clone, containing the V region of the TCR δ-chain, was expressed. Based on the above data, we concluded that 7G3 recognizes the C region of the TCR δ-chain.

3.3. Reactivity of 6F10 (CD8), 7G3 (TCR δ-chain) and 3E12 (γδ T-cells) in tissue sections

We next examined whether the newly established mAbs (6F10, 7G3, and 3E12) could be used for immunostaining on frozen sections. As shown in Fig. 7, all of the mAbs produced high-quality immunostaining results when used on frozen sections. In the thymus, 6F10 stained a significant number of both cortical and medullary thymocytes (Fig. 7). The strong staining pattern produced by 6F10 was striking when compared with the staining pattern produced by the commercially available CD8 α-chain mAb, the latter of which only weakly stained the thymocytes. Both 7G3 and 3E12 also stained small subpopulations of the thymocytes. $7G3^+$ cells were found mainly in the medulla, but a significant number of $7G3^+$ cells were also identified in the cortex of the thymus. In the medulla of the thymus, the $7G3^+$ cells tended to be found around Hassal's corpuscle. The $3E12^+$ cells were distributed in a similar manner as the $7G3^+$ cells, but the number of positive cells was lower than the number of $7G3^+$ cells. Commercially available mAbs against γδ T-cells were also examined, but none of these mAbs produced a satisfactory staining intensity. For example, mAb PGBL22A weakly stained only a small number of thymocytes. Similarly, the staining pattern produced by CD3 was not distinct on the frozen sections.

In lymph node (data not shown) and spleen tissues (Fig. 7), 6F10-stained cells were mainly distributed in the parafollicular area, which was rich in $CD2^+$ T-cells. In addition, a few $6F10^+$ cells were identified in the lymphoid follicles, which were visualized by the B-cell marker CD21 (data not shown). In the lymph node and spleen tissues, the $7G3^+$ and $3E12^+$ cells were scattered mainly in the parafollicular area.

4. Conclusions

In this paper, we report the development of a battery of murine mAbs that were reactive with porcine lymphocytes, including one Ab probably recognizes CD8 (6F10) and two anti-γδ T-cell Abs (7G3 and 3E12). All three of the newly characterized mAbs produced high-quality results when used for immunostaining on frozen sections, compared with the results obtained using commercially available anti-CD8 and anti-γδ T-cells mAbs.

The pig is unique with regard to the distribution of TCR in its peripheral organs. In mice and humans, from which a modern immunological scheme has been developed, the number of γδ T-cells in

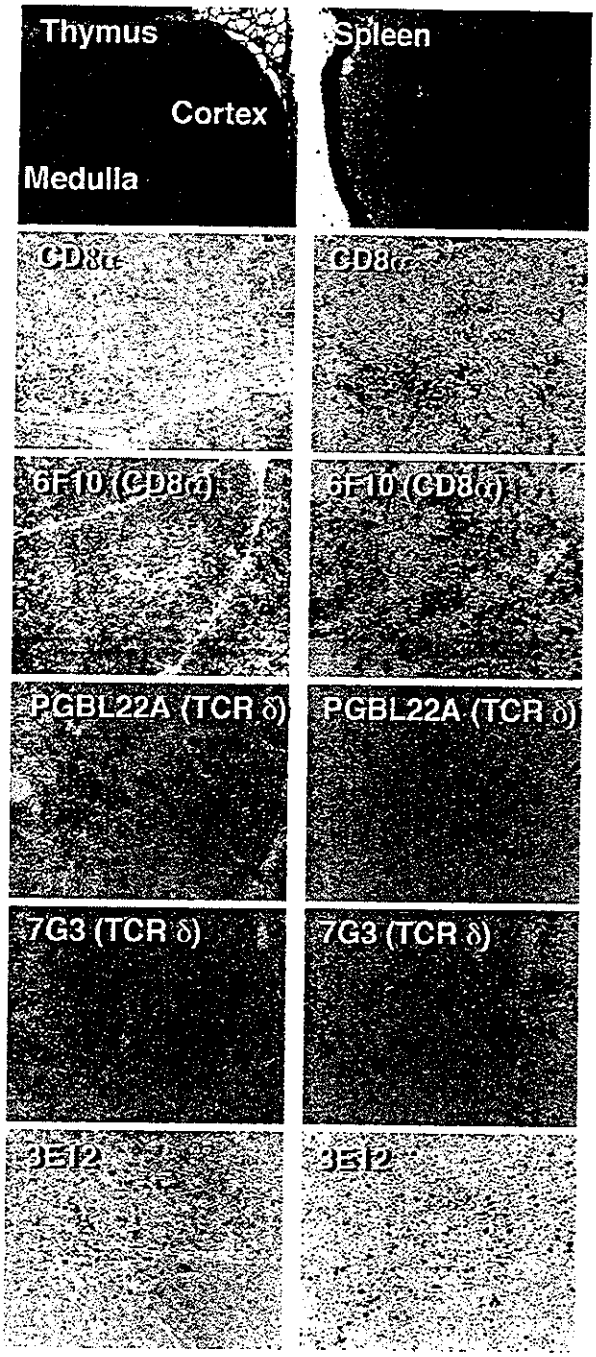

Fig. 7. Reactivity of 7G3, 3E12 and 6F10 on frozen sections of porcine tissues. Frozen sections of porcine thymus (left panels) and spleen (right panels) were stained with the monoclonal antibodies, as indicated.

peripheral lymphoid organs is very small, usually less than a few percent of the lymphocyte population (Carding and Egan, 2002). Instead, γδ T-cells tend to reside in the epithelia of various organs, such as the intestine, uterus and skin, that are often directly subjected to external Ag stimuli. Artiodactyls, including pig, however, are known to be abundant in γδ T-cells in their PB (Hein and Mackay, 1991). Davis et al., previously showed by using mAb PGBL22 that about 30–50% of porcine PB mononuclear cells are γδ T-cells (Davis et al., 1996, 1998, 2001). Indeed, five pigs we investigated also gave high proportion of γδ T-cells with an average of 24.7% with our new mAb 7G3, ranging from 16.1% to 32.7% and the value with PGBL22A was essentially the same with 7G3 in each pig. This striking feature prompted us to reconsider the biological role of γδ T-cells in defense immunity against direct Ag attacks from the external world. For this purpose, a precise characterization of porcine γδ T-cells, as well as αβ T-cells, is indispensable, and the data described here will serve to improve our understanding of the porcine immune system.

mAb 7G3 was selected based on its limited reactivity in PB lymphocytes and was found to react with a subpopulation of $CD3^+$ T-cells using two-color flow cytometry. Since this reactivity was quite similar to the previously reported proportion of γδ T-cells in porcine PB (Davis et al., 1998) we decided to compare our results with those obtained using established, commercially available mAbs. Among the mAbs against γδ T-cells that were tested, 7G3 exhibited a nearly identical distribution to that of mAb PGBL22A. The evidence that 7G3 immunoprecipated a protein with an identical molecular weight (approximately 40 kDa) to that produced by PGBL22A under reduced conditions further indicated that 7G3 and PGBL22A recognized the same molecule. In a previous report by another group, a biochemical analysis revealed that one TCR δ-chain with a molecular weight 40 kDa and three distinct TCR γ-chains with molecular weights of 37, 38, and 46 kDa were distributed in different subsets of porcine γδ T-cells (Hirt et al., 1990; Saalmuller et al., 1990; Thome et al., 1994). Based on the similarity of the identified molecular weights, we hypothesized that 7G3 reacts with the TCR δ-chain. To confirm this idea, we employed a molecular

biology approach. Fortunately, we were able to identify full-length cDNA clones of all TCR α-, β-, γ- and δ-chains in our cDNA libraries generated from 7G3$^+$ cells and 6F10$^+$ cells. Using a mammalian expression system, 7G3 was shown to react with Cos-7 cells in which all four TCR δ-chains cDNA had been introduced. Furthermore, 7G3 was shown to bind with a recombinant full-length TCR δ-chain protein fused with GST. These results confirmed that 7G3 reacts with the porcine TCR δ-chain.

Next, we investigated whether 7G3 reacts with the V or the C region of the porcine TCR δ-chain. Among the mAbs previously shown to react with γδ T-cells, PGBL22A seemed to have a wider range of reactivity than the other mAbs. PGBL22A was known to react with the TCR δ-chain, as proved using immunochemistry, but whether the mAb would react with a recombinant protein and the region of the TCR δ-chain that it recognized where uncertain. Using flow cytometry and various mAbs against porcine TCR γ-, δ-chains, the reactivities of 7G3 and PGBL22A were shown to be identical and were wider than those of the other mAbs. Thus, the possibility that both 7G3 and PGBL22A recognize a common framework in the TCR δ-chain (Davis et al., 1998, 2001) was considered, although the exact determinants are clearly different since these two mAbs can be used to perform a two-color analysis. The pig Vδ region sequences can be grouped into five families (Vδ1–5); one family, Vδ1, consists of a large number of members, whereas the other families have a limited number of members, as determined by cDNA sequencing as well as genomic Southern blotting (Yang et al., 1995). The TCR Vδ1 family was seen in 25 out of 34 cDNA clones in γδ T-cells obtained from a 1-month-old, germfree pig. In fact, four of the cDNAs for the TCR δ-chain found in the 7G3$^+$ cell cDNA library contained an identical V region (Vδ1), and the only differences were seen in the joint (J) region (Fig. 5). Therefore, 7G3 may recognize Vδ1, and not the C region, of the porcine TCR δ-chain. Consequently, we conducted an experiment to determine the region of the TCR δ-chain to which 7G3 reacts. Ideally, recombinant proteins of both the V region and the C region should have been produced, but we were only able to produce a GST-fusion TCR δ-chain mutant, in which the C region was completely deleted; this protein was unreactive with 7G3. These results does not necessary mean, however, that 7G3 does not bind TCR δ-chain V-domain because the folding of the V region peptide might be different from GST-fused full length TCR δ-chain in *Escherichia coli*.

We therefore attempted to use a mammalian expression system. Consistent with the results obtained using recombinant TCR δ-chain V-domain protein fused with GST, 7G3 did not reacted with the Cos-7 cells in which the expression vector for V region of the TCR δ-chain was transfected. It should be noted that the TCR δ-chain V region construct lacked membrane anchoring domain, and the peptides produced might be secreted out of Cos-7 cells. This experiment, therefore, cannot rule out the possibility of 7G3 binding to TCR δ-chain V-domain. We finally showed, however, that 7G3 clearly reacted with the Cos-7 cells in which the C region of the TCR δ-chain was expressed and the strength of staining with this construct was comparable to the Cos-7 cells with full length TCR δ-chain constructs. Taken together, the present evidence strongly suggest that at least a part of the epitope recognized by mAb 7G3 resides within the peptide coded by TCR δ-chain C region. Indeed, the published structure of a human γ δ TCR suggests a portion of TCR δ-chain C region to be accessible to antibody.

In this study, we also developed another mAb, 3E12, that reacts with a subset of γδ T-cells. Since the 3E12$^+$ subpopulation was always included in the population of 7G3$^+$ cells, namely the TCR δ-chain-expressing cells, and was never found in 7G3$^-$ cells, 3E12 likely recognizes a molecule expressed specifically on γδ T-cell subpopulation, but not the common framework of TCR γδ-chains. Furthermore, 3E12 did not react with the four TCR δ-chain proteins (TCR D1–4) or the one TCR γ-chain protein (TCR G) examined in this study. Comparing the reactivity of 3E12 and 7G3, it seems possible that 3E12 may recognize one of the three distinct TCR γ-chains other than one we cloned (Hirt et al., 1990; Saalmuller et al., 1990; Thome et al., 1994). Alternatively, 3E12 may recognize a Vδ family other than Vδ1 or a novel molecule related to the TCR γ- and δ-chain complex that is specifically expressed in a subset of γδ T-cells. A detailed investigation of the 3E12 Ag, including whether 3E12 recognizes the same molecule as that recognized by mAb PT79A, is now underway.

mAb 6F10 was found to react probably with the CD8 α-chain using flow cytometry. The major benefit of using 6F10 in research on the porcine immune system is its applicability to immunohistochemical analyses. Compared with the commercially available CD8 mAb, 6F10 reacts strongly on frozen sections. This benefit is also seen with the mAbs against γδ T-cells. mAb 7G3 distinctly stains TCR δ-chain$^+$ cells on frozen sections. Similarly, mAb 3E12 strongly stains a subset of γδ T-cells. Immunohistochemical analyses are particularly important for studying pathological conditions; thus, the mAbs developed in this study are expected to improve our understanding of not only the fundamental aspects of immune systems in general, but the immunological reactions involved in various porcine diseases.

In conclusion, we report the development of three mAbs that recognize distinct subsets of porcine T lymphocytes, all of which produced high-quality immunostaining results on tissue sections. In particular, mAb 7G3, which was confirmed to recognize the C region of the porcine TCR δ-chain, should facilitate the study of porcine γδ T-cells not only in the field of porcine immunity, but also in the field of comparative immunological evolution.

Acknowledgements

We thank M. Sone and S. Yamauchi for their excellent secretarial works. This work was supported in part by Health and Labour Sciences Research Grants and the Research Grant for Cardiovascular Disease from the Ministry of Health, Labour and Welfare of Japan and MEXT. KAKENHI 15019129, JSPS. KAKENHI 15390133 and 15590361. This work was also supported by a grant from the Japan Health Sciences Foundation for Research on Health Sciences Focusing on Drug Innovation. Additional support was provided by a grant from Sankyo Foundation of Life Science.

References

Carding, S.R., Egan, P.J., 2002. γδ T-cells: functional plasticity and heterogeneity. Nat. Rev. Immunol. 2, 336–345.

Davis, W.C., Brown, W.C., Hamilton, M.J., Wyatt, C.R., Orden, J.A., Khalid, A.M., Naessens, J., 1996. Analysis of monoclonal antibodies specific for the γδ TcR. Vet. Immunol. Immunopathol. 52, 275–283.

Davis, W.C., Zuckermann, F.A., Hamilton, M.J., Barbosa, J.I., Saalmuller, A.R., Binns, M., Licence, S.T., 1998. Analysis of monoclonal antibodies that recognize γδ T/null cells. Vet. Immunol. Immunopathol. 60, 305–316.

Davis, W.C., Haverson, K., Saalmuller, A., Yang, H., Lunney, J.K., Hamilton, M.J., Pescovitz, M.D., 2001. Analysis of monoclonal antibodies reacting with molecules expressed on γδ T-cells. Vet. Immunol. Immunopathol. 80, 53–62.

Fujimoto, J., Ishimoto, K., Kiyokawa, N., Tanaka, S., Ishii, E., Hata, J., 1988. Immunocytological and immunochemical analysis on the common acute lymphoblastic leukemia antigen (CALLA): evidence that CALLA on ALL cells and granulocytes are structurally related. Hybridoma 7, 227–236.

Haverson, K., Saalmuller, A., Alvarez, B., Alonso, F., Bailey, M., Bianchi, A.T., Boersma, W.J., Chen, Z., Davis, W.C., Dominguez, J., Engelhardt, H., Ezquerra, A., Grosmaire, L.S., Hamilton, M.J., Hollemweguer, E., Huang, C.A., Khanna, K.V., Kuebart, G., Lackovic, G., Ledbetter, J.A., Lee, R., Llanes, D., Lunney, J.K., McCullough, K.C., Molitor, T., Nielsen, J., Niewold, T.A., Pescovitz, M.D., de la Lastra, J.M., Rehakova, Z., Salmon, H., Schnitzlein, W.M., Seebach, J., Simon, A., Sinkora, J., Sinkora, M., Stokes, C.R., Summerfield, A., Sver, L., Thacker, E., Valpotic, I., Yang, H., Zuckermann, F.A., Zwart, R., 2001a. Overview of the third international workshop on swine leukocyte differentiation antigens. Vet. Immunol. Immunopathol. 80, 5–23.

Haverson, K., Saalmuller, A., Chen, Z., Huang, C.A., Simon, A., Seebach, J., Boersma, W.J., Zwart, R., Niewold, T.A., Thacker, E., Llanes, D., de la Lastra, J.M., Engelhardt, H., Ezquerra, A., Alonso, F., Dominguez, J., Ledbetter, J.A., Grosmaire, L., Lee, R., Nielsen, J., Salmon, H., Valpotic, I., Sver, L., Lackovic, G., Summerfield, A., Khanna, K.V., 2001b. Summary of the first round analyses of the third international workshop on swine leukocyte differentiation antigens. Vet. Immunol. Immunopathol. 80, 25–34.

Hein, W.R., Mackay, C.R., 1991. Prominence of γδ T-cells in the ruminant immune system. Immunol. Today 12, 30–34.

Hirt, W., Saalmuller, A., Reddehase, M.J., 1990. Distinct γ/δ T-cell receptors define two subsets of circulating porcine CD2–CD4–CD8–T lymphocytes. Eur. J. Immunol. 20, 265–269.

Maruyama, K., Sugano, S., 1994. Oligo-capping: a simple method to replace the cap structure of eukaryotic mRNAs with oligoribonucleotides. Gene 138, 171–174.

Saalmuller, A., Hirt, W., Reddehase, M.J., 1990. Porcine γ/δ T lymphocyte subsets differing in their propensity to home to lymphoid tissue. Eur. J. Immunol. 20, 2343–2346.

Takada, K., Saito, M., Kaneko, H., Iizuka, K., Kokai, Y., Fujimoto, J., 1995. Novel monoclonal antibody reactive with thrombin-sensitive 74-kDa glycoproteins present on platelets and megakaryocytes both from mouse and rat. Hybridoma 14, 361–367.

Thome, A., Saalmuller, A., Pfaff, E., 1993. Molecular cloning of porcine T-cell receptor alpha, beta, gamma and delta chains using polymerase chain reaction fragments of the constant regions. Eur. J. Immunol. 23, 1005–1010.

Thome, M., Hirt, W., Pfaff, E., Reddehase, M.J., Saalmuller, A., 1994. Porcine T-cell receptors: molecular and biochemical characterization. Vet. Immunol. Immunopathol. 43, 13–18.

Yang, Y.-G., Ohta, S., Yamada, S., Shimizu, M., Takagaki, Y., 1995. Diversity of T-cell receptor δ-chain cDNA in the thymus of a 1-month-old pig. J. Immunol. 155, 1981–1993.

Shiga toxin binding to globotriaosyl ceramide induces intracellular signals that mediate cytoskeleton remodeling in human renal carcinoma-derived cells

Hisami Takenouchi[1,2], Nobutaka Kiyokawa[1,*], Tomoko Taguchi[1], Jun Matsui[1], Yohko U. Katagiri[1], Hajime Okita[1], Kenji Okuda[2] and Junichiro Fujimoto[1]

[1]Department of Developmental Biology, National Research Institute for Child Health and Development, 3-35-31, Taishido, Setagaya-ku, Tokyo, 154-8567, Japan

[2]Department of Bacteriology, Yokohama City University School of Medicine, 3-9 Fukuura, Kanazawa-ku, Yokohama 236-0004, Japan

*Author for correspondence (e-mail: nkiyokawa@nch.go.jp)

Accepted 6 April 2004
Journal of Cell Science 117, 3911-3922 Published by The Company of Biologists 2004
doi:10.1242/jcs.01246

Summary

Shiga toxin is a bacterial toxin consisting of A and B subunits. Generally, the essential cytotoxicity of the toxin is thought to be mediated by the A subunit, which possesses RNA cleavage activity and thus induces protein synthesis inhibition. We previously reported, however, that the binding of the Shiga toxin 1-B subunit to globotriaosyl ceramide, a functional receptor for Shiga toxin, induces intracellular signals in a manner that is dependent on glycolipid-enriched membrane domains, or lipid rafts. Although the precise role of this signaling mechanism is not known, here we report that Shiga-toxin-mediated intracellular signals induce cytoskeleton remodeling in ACHN cells derived from renal tubular epithelial carcinoma. Using confocal laser scanning microscopy, we observed that Shiga toxin 1-B treatment induces morphological changes in ACHN cells in a time-dependent manner. In addition, the morphological changes were accompanied by the redistribution of a number of proteins, including actin, ezrin, CD44, vimentin, cytokeratin, paxillin, FAK, and α- and γ-tubulins, all of which are involved in cytoskeletal organization. The transient phosphorylation of ezrin and paxillin was also observed during the course of protein redistribution. Experiments using inhibitors for a variety of kinases suggested the involvement of lipid rafts, Src family protein kinase, PI 3-kinase, and RHO-associated kinase in Shiga toxin 1-B-induced ezrin phosphorylation. Shiga toxin 1-B-induced cytoskeletal remodeling should provide an in vitro model that can be used to increase our understanding of the pathogenesis of Shiga-toxin-mediated cell injury and the role of lipid-raft-mediated cell signaling in cytoskeletal remodeling.

Key words: Shiga toxin, Globotriaosylceramide, Cytoskeleton

Introduction

Shiga toxin (Stx) is a protein toxin produced by Stx-producing strains of *Escherichia coli* (STEC) and has been postulated to be the substance responsible for the development of serious complications associated with STEC infection, such as hemolytic uremic syndrome (HUS) (Kaplan et al., 1990; Richardson et al., 1988). Stx consists of two major types, Stx1 and Stx2, that both contain an A-subunit monomer and a B-subunit pentamer (Lingwood, 1996). The A-subunit is a 30 kDa cytotoxic chain that exhibits RNA *N*-glycohydrolase activity and cleaves a specific adenine residue on the 28S ribosomal RNA in the cytosol, thereby inhibiting protein synthesis (Lingwood, 1996). In contrast, the 7 kDa B-subunit can bind to globotriaosyl ceramide (Gb3), the functional receptor for Stx found on the surface of target cells (Lingwood, 1996). Although Stx cytotoxicity is thought to be caused by the A-subunit-mediated inhibition of protein synthesis, a number of recent studies have clarified that the B-subunit also has a biological effect on the target cells.

For example, Stx-B binding to Gb3 has been shown to trigger intracellular signaling events in Burkitt's lymphoma cells (Taga et al., 1997). We further observed that Gb3 was only distributed in glycolipid-enriched membrane (GEM) domains (Rodgers and Rose, 1996), also known as lipid rafts (Simons and Ikonen, 1997), indicating that lipid rafts are deeply involved in Stx-mediated signal transduction in both Burkitt's lymphoma cells (Mori et al., 2000) and renal carcinoma ACHN cells (Katagiri et al., 1999). However, the physiological role of Gb3-mediated cell signaling remains unknown. Although Stx1-B binding is sufficient to induce apoptosis in Burkitt's lymphoma cells (Kiyokawa et al., 2001; Mangeney et al., 1993; Taga et al., 1997), this effect of Stx1-B appears to be limited to this species of cells, and the A-subunit of Stx is reportedly required to induce apoptosis in other cell types, including Vero cells and monocytic THP-1 cells (Kojio et al., 2000; Williams et al., 1997).

Ezrin, radixin and moesin are members of the ERM protein family and are mainly distributed just beneath the plasma membranes of cellular protrusions, such as microvilli. ERM proteins are thought to function as general cross-linkers between plasma membranes and actin filaments (Arpin et al., 1994; Bretscher et al., 1997; Tsukita and Yonemura, 1997; Tsukita et al., 1997; Tsukita and Yonemura, 1999). The highly conserved NH2-terminal halves of ERM proteins possess the

ability to associate with several integral membrane proteins, such as CD43, CD44, intercellular adhesion molecule (ICAM)-1, ICAM-2, ICAM-3, and the H^+/K^+ ATPase pump (Bretscher et al., 1997; Heiska et al., 1998; Hirao et al., 1996; Serrador et al., 1997; Tsukita et al., 1994; Tsukita and Yonemura, 1999; Yonemura et al., 1993). Conversely, the COOH-terminal halves of ERM proteins can interact with actin filaments (Bretscher et al., 1997; Tsukita and Yonemura, 1999; Turunen et al., 1994). As the NH2-terminal halves of ERM proteins can also bind to their COOH-terminal halves (Andreoli et al., 1994; Bretscher et al., 1997; Tsukita and Yonemura, 1999), both the actin- and membrane-binding domains of ERM proteins are thought to be masked in the resting state by an intramolecular and/or intermolecular head-to-tail association (Berryman et al., 1995; Bretscher et al., 1995; Bretscher et al., 1997; Tsukita and Yonemura, 1999). These dormant ERM proteins are thought to be activated by cellular signals, such as the one mediated by epidermal growth factor receptor, by exposing their halves and allowing them to interact with integral membrane proteins and actin filaments, respectively (Berryman et al., 1995; Bretscher et al., 1995; Bretscher et al., 1997; Hirao et al., 1996; Matsui et al., 1998; Tsukita and Yonemura, 1999). These activated ERM proteins have been shown to be directly involved in the morphogenesis of the free surface domain of plasma membranes, especially in the organization of microvilli (Berryman et al., 1995; Bretscher et al., 1997; Chen et al., 1995; Crepadi et al., 1997; Kondo et al., 1997; Takeuchi et al., 1994; Tsukita and Yonemura, 1999).

In this study, we investigated the effect of Stx1-B binding to Gb3 on ACHN cells and found that an intracellular signal mediated by Gb3 induces the phosphorylation of ezrin proteins, leading to a reorganization of the cytoskeleton and morphological changes. Our findings should improve our understanding of the molecular mechanism of Stx-mediated cell damage and the functional roles of Gb3-mediated intracellular signals in a physiological context.

Materials and Methods

Materials

The Stx1-B pentamer was prepared as described previously (Nakajima et al., 2001). The mouse monoclonal antibodies (mAbs) used in this study were obtained from BD Biosciences (Lexington, KY) (anti-ezrin, anti-paxillin and anti-Yes), Immunotech (Fullerton, CA) (anti-CD44 and anti-cytokeratin), Affinity BioReagents, Inc. (ABR, Golden, CO) (anti-vimentin), Santa Cruz Biotechnology (Santa Cruz, CA) (anti-actin), and Sigma-Aldrich Fine Chemicals (St Louis, MO) (anti-α Tubulin). The mouse anti-Gb3 mAb 1A4 was a generous gift of S. Hakomori of the University of Washington (Seattle, WA) and Otsuka Assay Laboratories (Kawauchi-cho, Tokushima, Japan). The rat anti-Gb3 mAb 38.13 were obtained from Immunotech. The polyclonal Abs were obtained from Upstate biotechnology (Lake Placid, NY) (anti-FAK), New England Biolabs, (Bevely, MA) (anti-phospho-specific ezrin and anti-phospho-specific paxillin), ABR (anti-phospho-specific Src) and Sigma (anti-γ Tubulin). Peroxidase-conjugated secondary Abs were purchased from DAKO (Glostrup, Denmark). Fluorescence-conjugated secondary Abs and fluorescence labeling reagents for the primary Abs were purchased from Molecular Probes, Inc. (Eugene, OR). The Rho-dependent serine/threonine kinase (ROCK) inhibitor Y-27632, PI 3 kinase (PI3K) inhibitor LY-294002, protein kinase C (PKC) inhibitor 20-28, PKC inhibitor EGF-R fragment 651-658, and Src family protein tyrosine kinase (PTK) inhibitor PP2 were purchased from Calbiochem-Novabiochem (San Diego, CA). Methyl-β-cyclodextrin (MBD) and DAPI were obtained from Sigma. TRITC-conjugated phalloidin was purchased from Molecular Probes. Cell-tracker Green was also purchased from Molecular Probes. Other chemical reagents were obtained from Wako Pure Chemical Industries (Osaka, Japan), unless otherwise indicated.

Cell culture

Renal tubular epithelial carcinoma-derived ACHN cells that were sensitive to Stx1 cytotoxicity (Katagiri et al., 1999; Taguchi et al., 1998) were used in this study. The cells were maintained in DMEM supplemented with 10% FCS at 37°C in a humidified 5% CO_2 atmosphere. Cells were grown to approximately 75% confluence and stimulated. In most of the experiments, Stx1-B pentamer was directly added to the culture medium at a concentration of 5.0 μg/ml and cells were incubated for the time periods indicated in the figures, unless otherwise indicated.

Immunohistochemistry and confocal microscopic analysis

To observe cell morphology, ACHN cells were plated on a polylysine-coated glass bottom dish (Matsunami Glass, Tokyo, Japan) and labeled with Cell-tracker Green, according to the manufacturer's protocol. For the immunohistochemical staining, the cells were plated on a collagen-coated cover slip (Iwaki Glass, Tokyo, Japan). After each treatment, cells on cover slips were washed with ice–cold PBS and fixed with ice-cold acetone for 20 minutes at 4°C, then stained with each combination of Abs and/or reagents described below.

For the simultaneous detection of ezrin and filamentous actin (F-actin), the cover slips were incubated with primary Abs against ezrin (5 μg/ml) at room temperature for 30 minutes followed by PBS washing. The cells were further incubated with secondary goat anti-mouse Ab labeled with Alexa Fluor® 488 (1:300 dilution) for 30 minutes, followed by PBS washing and then stained with DAPI (200 ng/ml) and TRITC-conjugated phalloidin (5 units/ml) (Knowles and McCulloch, 1992). The detection of CD44 and F-actin was performed similarly.

For the detection of paxillin and FAK, a combination of mouse anti-paxillin mAb and rabbit anti-FAK polyclonal Ab was used. Both primary Abs (5 μg/ml each) were detected by Alexa Fluor® 488-conjugated goat anti-mouse Ab and Alexa Fluor® 546-conjugated goat anti-rabbit Ab (1:300 each), respectively. Each secondary Ab was highly cross-absorbed, thus the cross reactions were not detected in preliminary experiments (data not shown). The detection of α- and γ-tubulin was performed similarly. For the simultaneous detection of vimentin and cytokeratin, each primary Ab was labeled using either the Alexa Fluor® 488 Protein Labeling Kit or the Zenon™ Alexa Fluor® 546 Mouse IgG1 Labeling Kit.

Confocal laser scanning was performed using a FV500 confocal laser scanning microscope (Olympus, Tokyo, Japan). Simultaneous multi-fluorescence acquisitions were performed using the 351 nm, 488 nm, and 543 nm laser lines to excite DAPI, Alexa Fluor™488, and Alexa Fluor™546 (TRITC), respectively, using a water-immersion objective (×40, NA1.7). Fluorescent images were selected using appropriate multi-fluorescence dichroic mirrors and band pass filters using the sequential acquisition mode.

Immunoblot analysis

For the immunoblot analysis, ACHN cells were plated on a 100 mm culture dish (Corning, Corning, NY). Cell lysates were prepared by solubilizing cells in 400 μl of lysis buffer, and the protein concentration of each cell lysate was determined as described previously (Kiyokawa et al., 2001). 50 μg of each whole cell lysate was electrophoretically separated on an SDS-polyacrylamide gel and transferred to a nitrocellulose membrane using a semi-dry transblot

system (Bio-Rad Laboratories, Hercules, CA). Immunoblotting was performed as described previously (Kiyokawa et al., 2001).

Actin and tubulin polymerization assay

Quantification of actin polymerization was carried out essentially as described previously with minor modifications (Heacock and Bamburg, 1983; Glogauer et al., 1997; McCormack et al., 1999). Briefly, ACHN cells were plated in quintuple wells of a 6-well culture dish (Corning) at 1.5×10^5 cells in 5 ml of medium, and grown for 40 hours to achieve approximately 75% confluence, and treated with 5.0 μg/ml of Stx1-B pentamer for the time periods indicated in the figures. At the end of the incubation period, cells were washed in ice-cold PBS and quickly lysed in 500 μl of actin stabilization buffer (Heacock and Bamburg, 1983; McCormack et al., 1999), a buffer that stabilizes both monomer actin (G-actin, soluble) and F-actin (polymerized) pools. Aliquots of 50 μl from each original (whole) lysate were removed and stored for the determination of total actin. The cell lysates were immediately centrifuged at room temperature for 1 minute in a microcentrifuge at 10,000 *g*, after which the supernatants (G-actin) were removed from the pellets (F-actin). Then 450 μl of actomyosin extraction buffer (Heacock and Bamburg, 1983) was added to the solid pellets. Aliquots of 5 μl from both original lysates (total actin) and resuspended pellets (F-actin) were examined by immunoblot analysis using anti-actin mAb and quantified by densitometry (Glogauer et al., 1997). The proportion of F-actin to total actin was calculated and shown as a percentage.

Quantification of tubulin polymerization was examined essentially the same as actin polymerization with some exceptions. First, the original lysates were prepared by using specific lysis buffer for tubulin and centrifuged at 10,000 *g* for 10 minutes as described elsewhere (Minotti et al., 1991; Montgomery et al., 2000). Second, after removal of the supernatants containing soluble tubulin, solid pellets containing polymerized tubulin were resuspended in water (Minotti et al., 1991; Montgomery et al., 2000). Third, immunoblot analysis was performed with anti-α tubulin mAb.

Results

Morphological changes in ACHN cells induced by Stx1-B treatment

We previously observed, during a study on the biological function of the Stx1-B subunit, that Stx1-B treatment induces a weakening in the adhesion of ACHN cells to the culture dish (Katagiri et al., 2001). As the same phenomenon is also observed in primary cultures of normal human renal cortical epithelial cells (data not shown), it is likely that this is a common feature observed in renal epithelial-derived cells mediated by Stx1-B-induced intracellular signals.

To examine the effect of Stx1-B on the adhesiveness of ACHN cells in greater detail, we stained the cells with Cell-tracker Green and observed the morphological changes using confocal laser scanning microscopy. As shown in Fig. 1, the addition of Stx1-B to the culture weakened the adhesiveness of the cells, as recognized by the increase in intracellular spaces in a time-dependent manner and by the morphological changes, in which the cells became smaller and rounder. In addition, filopodia- and lamellipodia-like structures were temporarily observed after Stx1-B treatment (Fig. 1, arrowhead).

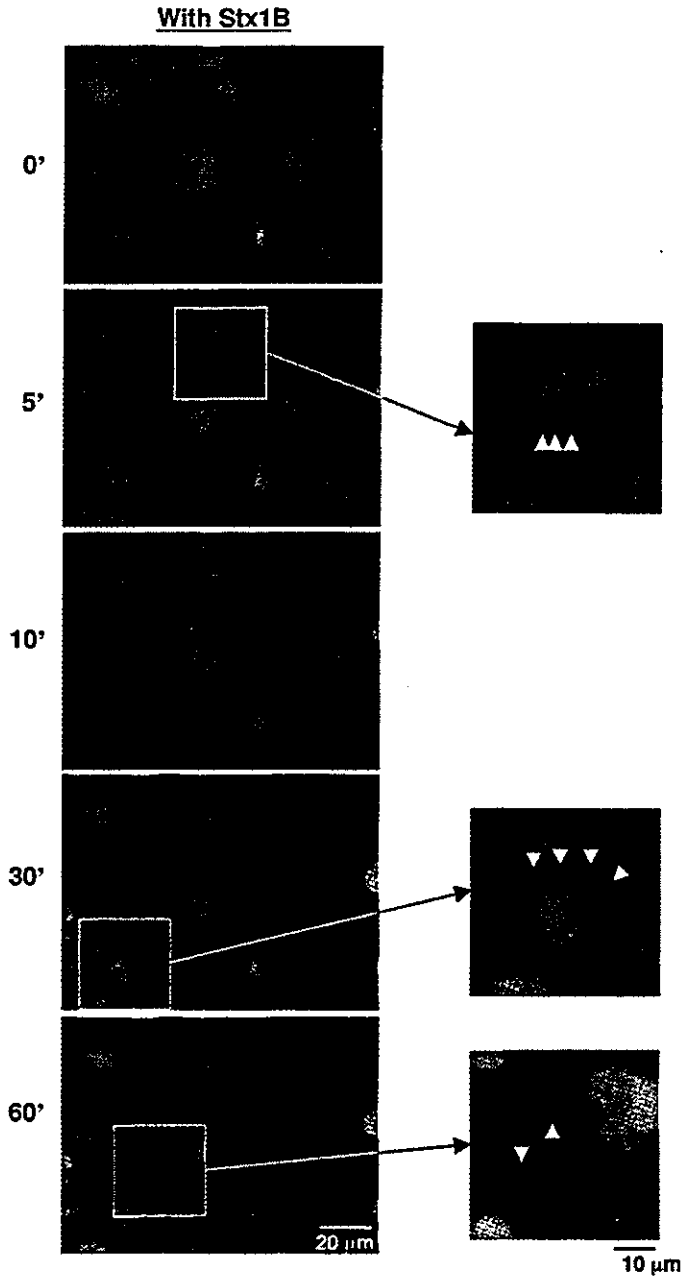

Fig. 1. Morphological changes in ACHN cells after treatment with the Stx1-B subunit. ACHN cells stained with Cell-tracker Green were treated with and without 5 μg/ml of the Stx1-B subunit for the indicated periods and visualized using confocal microscopy. Filopodia- and lamellipodia-like structures are visible at higher magnifications and are indicated by the arrowheads. Results are representative of three independent experiments.

Stx1-B induces the redistribution of cytoskeletal proteins in ACHN cells

The remodeling of cytoskeletal proteins, including the ERM family proteins and actin, is involved in the formation of filopodia or lamellipodia during morphological changes (Berryman et al., 1995; Bretscher et al., 1997; Chen et al., 1995; Crepadi et al., 1997; Kondo et al., 1997; Takeuchi et al., 1994; Tsukita and Yonemura, 1999). Therefore, we examined whether Stx1-B treatment affects the distribution of ezrin and actin. In the resting state, most of the ezrin protein was dispersed in the cytoplasm and only a portion of the protein